Biochemistry

 Volume 37, Number 19 May 12, 1998

Articles

Interfacial Activation of Triglyceride Lipase from *Thermomyces (Humicola) lanuginosa*: Kinetic Parameters and a Basis for Control of the Lid†

Otto G. Berg,‡ Yolanda Cajal,§ Glenn L. Butterfoss,|| Ronald L. Grey,|| M. Asuncion Alsina,§ Bao-Zhu Yu,|| and Mahendra K. Jain*,||

Department of Chemistry and Biochemistry, University of Delaware, Newark, Delaware 19716, Physical Chemistry Unit, Facultad de Farmacia, University of Barcelona, Barcelona, Spain, and Department of Molecular Biology, Uppsala University Biomedical Center, Uppsala, Sweden

Received December 5, 1997; Revised Manuscript Received March 3, 1998

ABSTRACT: A strategy is developed to analyze steady-state kinetics for the hydrolysis of a soluble substrate partitioned into the interface by an enzyme at the interface. The feasibility of this approach to obtain interfacial primary kinetic and equilibrium parameters is demonstrated for a triglyceride lipase. Analysis for phospholipase A_2 catalyzed hydrolysis of rapidly exchanging micellar (Berg et al. (1997) *Biochemistry 36*, 14512−14530) and nonexchangeable vesicular (Berg et al., (1991) *Biochemistry 30*, 7283−7291) phospholipids is extended to include the case of a substrate that does not form the interface. The triglyceride lipase (tlTGL) from *Thermomyces (formerly Humicola) lanuginosa* hydrolyzes *p*-nitrophenylbutyrate or tributyrin partitioned in the interface of 1-palmitoyl-2-oleoyl-*sn*-glycero-3-phosphoglycerol (POPG) vesicles at a rate that is more than 100-fold higher than that for the monodispersed substrate or for the substrate partitioned into zwitterionic vesicles. Catalysis and activation is not seen with the S146A mutant without the catalytic serine-146; however, it binds to the POPG interface with the same affinity as the WT. Thus POPG acts as a diluent surface to which the lipase binds in an active, or "open", form for the catalytic turnover; however, the diluent molecules have poor affinity for the active site. Analysis of the substrate and the diluent concentration dependence of the rate of hydrolysis provides a basis for the determination of the primary interfacial catalytic parameters. As a competitive substrate, tributyrin provided a check for the apparent affinity parameters. Nonidealities from the fractional difference in the molecular areas in interfaces are expressed as the area correction factor and can be interpreted as a first-order approximation for the interfacial activity coefficient. The basis for the interfacial activation of tlTGL on anionic interface is attributed to cationic R81, R84, and K98 in the "hinge" around the 86−93 "lid" segment of tlTGL.

Secreted phospholipase A_2 has served as a useful prototype for developing current knowledge of interfacial catalysis (*1*−*3*). Aided by crystal structures (*4*−*6*) and site-directed mutagenesis (*7*−*9*), the knowledge of the primary rate and equilibrium constants (*10*−*13*) for secreted phospholipase A_2 has allowed significant insights into interfacial catalysis (*2*, *3*) and activation (*11*, *12*). Such detailed analysis of phospholipase A_2 in terms of the primary interfacial kinetic

† This work was supported by PHS (GM29703 to M.J.) and the Swedish Natural Science Research Council (to O.B.). Summer support for G.B. was provided by the Undergraduate Biological Sciences Education Program from the Howard Hughes Medical Institute.

* Corresponding author.
‡ Uppsala University.
§ University of Barcelona.
|| University of Delaware.

S0006-2960(97)02998-X CCC: $15.00
Published on Web 04/22/1998

Scheme 1: A Kinetic Model for Interfacial Catalysis and Activation[a]

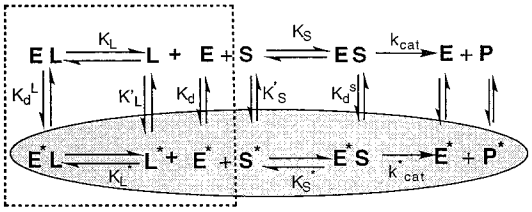

[a] The species marked with an asterisk are in the interface and are in equilibrium with the corresponding species in the aqueous phase. The equilibrium dissociation constants have their standard definitions. Dissociation constants marked with an asterisk, expressed in units of mole fraction, represent two-dimensional equilibria. L could be an inhibitor (K_I*), a competitive substrate (K_M*), or an imperfect diluent (K_{ND}*). K_M* and k^*_{cat} represent the interfacial turnover parameters. Results show that turnover through k_{cat} is <1% of the interfacial rate. Complete analysis of the model is developed in the appendix for the conditions where the enzyme, substrate, and products of hydrolysis equilibrate so that the chemical step is rate limiting. For the significance of this scheme in the general context of interfacial kinetics, see refs *2*, *10*, and *11*.

and equilibrium parameters has been possible because the phospholipid aggregates spontaneously form interfaces with well-defined composition, organization, and exchange dynamics. In this study we extend this experience, as formalized in the kinetic Scheme 1 (*11*), to establish conditions for the analysis of interfacial catalysis and activation by a triglyceride lipase.

Lipases (triglyceride hydrolases) as a class are probably the second best structurally characterized group of interfacial enzymes (*14*−*18*); however, the functional significance of many of their interesting structural features remains to be established. A major difficulty lies in the fact that the polymorphism and organizational state of triglycerides in the aqueous dispersions are difficult to control. Triglycerides are virtually insoluble in water because they are essentially nonpolar with a very weak amphiphilic character. If suspended in water, they adsorb onto the available surfaces or form droplets of uncontrolled dispersity. Inability to form organized interfaces with triglycerides makes it nearly impossible to generate well-defined structures of known surface area and measurable exchange rates between the coexisting interfaces. Use of sparingly soluble substrates, such as tributyrin or *p*-nitrophenylbutyrate (PNPB)[1] below their bulk solubility limit, for kinetic measurements appears to be limited by the reaction at other interfaces. The solubility of tributyrin is about 0.8 mM; however, below this concentration one cannot be certain that the catalysis occurs solely through the monomers in the solution via monodisperse Michaelis complexes. Not only may the complex with the enzyme be in a microaggregate form, but the hydrolysis may occur at interfaces offered by air bubbles or the reaction vessel. Since it is difficult to establish whether the hydrolysis observed below the solubility limit is at interfaces or truly with monodispersed substrate molecules, in one of the most commonly used assays tributyrin is used in a frothy emulsion stabilized by gum arabic (*19*, *20*). It is not surprising that such assays are not useful for the kinetic analysis in terms of the primary rate and equilibrium constants, and the lipase kinetics remains unresolved.

In this study we report the theory and protocols to analyze the interfacial catalysis by a triglyceride lipase from *Thermomyces lanuginosa* (tlTGL). As outlined in Scheme 1, the observed hydrolysis in the presence of an interface is the sum of the turnover in the aqueous phase and in the interface. Besides the knowledge of the binding of the enzyme to the interface and of the specific steps involved in the catalytic turnover at the interface, this analysis also requires an understanding of the solubility and partitioning equilibria for the substrate and the enzyme (Appendix). The situation is considerably simplified because the hydrolysis by tlTGL occurs predominantly via the interfacial path, and the substrate and product exchange rate between the aqueous phase and the interface is rapid. Thus, on the basis of the assumption of a diffusion-limited on-rate for the binding of the substrate to the interface, the substrate replenishment rate is expected to be rapid for solutes with >1 μM solubility in water.

In Scheme 1 the binding of the enzyme to the interface, the E to E* step, is distinct from the steps of the catalytic turnover at the interface. A primary task for the kinetic analysis developed in Appendix is to develop a well-defined interface of the diluent (ND) molecule, which must satisfy several criteria: the enzyme bound to the interface must not bind the diluent molecules to the active site; however, E* must bind and catalyze the hydrolysis of substrate molecules partitioned in the ND interface. As the substrate molecules partition in the diluent interface, the interfacial substrate concentration, X_S, determines the E* + S to E*S equilibrium. Analysis is simplified considerably if the rate of substrate replenishment and the product release are rapid so that the chemical step, k^*_{cat}, remains rate-limiting. Thus the effective interfacial catalytic turnover rate will be given by the steps shown in the shaded oval by species marked with an asterisk.

In this study we show the analytical feasibility of Scheme 1 to determine the interfacial kinetic parameters for tlTGL. Specifically, the rate of hydrolysis of PNPB or tributyrin by tlTGL is enhanced over 100-fold at the interface of POPG vesicles. Results are consistent with the catalytic role for the consensus catalytic triad (*21*) because the S146A mutant of tlTGL is catalytically inert. The analysis developed in Appendix provides a basis for obtaining values of the interfacial Michaelis−Menten parameters (K_M* and k^*_{cat}), the dissociation constant of the enzyme at the interface (K_d), and the partition coefficient of the substrate in the interface (K_S'). Results show that POPG is a good diluent with a poor affinity for the active site of the bound enzyme, possibly with K_{ND}* > 1 mol fraction. The spectroscopic properties of the S146A tlTGL mutant show a change in the environment of tryptophan residue(s), which provides complementary information about the interfacial binding event. Comparable kinetic behavior is observed with pig pancreatic lipase. These results are interpreted to suggest that the interfacial activation of tlTGL on anionic POPG, but not on zwitterionic vesicles, is controlled through the cationic

[1] Abbreviations: Cmc, critical micelle concentration; HDNS, *N*-dansylhexadecylphosphoethanolamine; ND, a surface diluent such as POPG.; PNPB, *p*-nitrophenylbutyrate; POPC, 1-palmitoyl-2-oleoyl-*sn*-glycero-3-phosphocholine; POPG, 1-palmitoyl-2-oleoyl-*sn*-glycero-3-phosphoglycerol; RET, resonance energy transfer; TB, tributyrin or tributyroylglycerol; tlTGL triglyceride lipase from *Thermomyces lanuginosa*.

residues in the "hinge" region around the "lid" on the catalytic site.

MATERIAL AND METHODS

PNPB and TB were from Sigma, and phospholipids were from Avanti Polar Lipids. HDNS was prepared as described (*22*). Most of the calculations and data fits for linear or hyperbolic relations were carried out with the Inplot 4 program; however, the fits for more complex relations were generated and evaluated through the Math-Cad program. Typically, uncertainty in the primary experimental results is <10%, and the uncertainty in the derived curve-fitting parameters is estimated to be 30% as the standard deviation.

Purified tlTGL from *Thermomyces lanuginosa* and its S146A mutant, in which the catalytic serine is changed to alanine, were kindly provided by Dr. Allan Svendsen of NovoNordisk, Denmark (*18*). The aqueous solutions of the enzyme tend to lose some activity, presumably due to aggregation, on lyophilization and freezing−thawing, or even after long incubations at 4 °C. For kinetic studies and calibrations we chromatographed the enzyme by gel filtration on an HPLC column (Bio-Rad TSK-250). In this preparation the ratio of ODs at 280 and 260 nm was 3.94 compared to the ratio of 1.7 seen before the purification. For the calculation of enzyme concentration, the molar extinction coefficient of 43 000 M^{-1} cm^{-1} (*23*) was used, with molecular mass = 32 kDa.

Vesicles. Small unilamellar vesicles of POPG or POPC were prepared by hydration of the vacuum-dried lipid film and sonication in a bath-type sonicator (Lab Supplies, Hickesville, NY, model G112SPIT) until a clear dispersion was obtained. HDNS (2.5 mol %) was incorporated in the preformed vesicles by adding an aliquot of vesicles to a glass tube with a vacuum-dried film of HDNS, followed by mixing and incubation for 30 min in the dark. Vesicles were annealed for 1 h above their transition temperature.

Kinetic Protocols. Hydrolysis of PNPB was monitored as the change in the optical density (OD) at 400 nm, corresponding to the absorption maximum of *p*-nitrophenolate anion with a molar extinction coefficient of 14 000 (Figures 1 and 3). Data acquisition and manipulation were carried out on Hewlett-Packard diode array spectrophotometer with a 0.5-s acquisition time. These measurements were carried out in 0.7 mL of 10 mM Tris at pH 8.0 and 25 °C in a quartz cuvette. PNPB was added from a stock solution in tetrahydrofuran or ethanol. POPG vesicles, specified as the total lipid concentration, were used to provide an interface for the enzyme to bind and adopt an "open", or interface-active, conformation to which the substrate can bind. The reaction was initiated by the addition of 5−30 pmol of the enzyme, and the hydrolysis commenced less than 5 s after the addition. The contents of the cuvette were mixed 7−10 times by gentle inversion of the cuvette capped with Parafilm, and the contents were left unstirred during the course of the measurement. As shown later, this precaution is necessary because vigorous stirring of the solution creates bubbles or turbulence that provide an air−water interface for the partitioning of the substrate and enzyme. Such factors are not controllable, and they lead to an overestimate of the observed rate. For comparative purposes some kinetic measurements were also made by pH-stat protocol (*10*, *11*, *24*); however, the surface of the vessel and air bubbles make it unsuitable for detailed kinetic analysis in the absence of added diluent. Reliable rates by pH-stat could be estimated only in the presence of excess diluent. Hydrolysis of TB was also independently monitored by pH-stat methods in the presence of POPG vesicles.

The rate, calculated from the slope of the initial zero-order phase of the progress curve, is expressed as turnover number per second. The background OD drift without the enzyme was negligible (<1%) compared to the observed rate.

Substrate Competition. Inhibition of the hydrolysis of PNPB by TB was determined by the spectrophotometric protocol. Increasing concentrations of TB were added to the mixture containing 0.353 mM PNPB and 0.0534 mM POPG, and the reaction was initiated by addition of tlTGL (1−50 pmol, depending on the conditions). Data were expressed as $v_o/v_I - 1$, where v_o and v_I are the rate of hydrolysis in the absence and in the presence of TB, respectively (Figure 6).

Maximum Solubility. The solubility limit for PNPB was determined as the change in the 90° scattering intensity at 500 nm with 1-nm slit widths on an SLM-Aminco AB2 spectrofluorimeter (Figure 2). PNPB was added from a 24.7 mM stock solution in tetrahydrofuran to a cuvette containing 1.4 mL of 10 mM Tris buffer at pH 8.0 and 25 °C. The solubility limit for TB was also determined by the scattering, as well as by monitoring the increase in the fluorescence emission of diphenylhexatriene as it partitions into droplets of TB. The change in the scattering above the solubility limit of PNPB or TB was also monitored in the presence of POPG. In these cases the scattering from vesicles changes modestly as the solute partitions, and a more abrupt change in the scattering is observed above the solubility limit.

Partitioning of PNPB. The partitioning of PNPB in POPG vesicles was monitored as a function of the lipid concentration (Figure 4A). POPG vesicles in 0−5.16 mM final concentration were added from a 26.7 mM stock solution to a series of tubes containing 0.28 mM PNPB in a 0.62-mL final volume of 10 mM Tris at pH 8.0 and 24 °C. The solutions were filtered at 24 °C through 30 000-cutoff Centricon filters by centrifugation at 5500 rpm in a Servoll centrifuge. The filtrate containing free PNPB was recovered, and the optical density at 274 nm was measured. Results are plotted as percent PNPB bound = $100(OD_{total} - OD_{free})/OD_{total}$, where OD_{free} is the absorption of the filtrate in the presence of POPG, and OD_{total} is the reading in the absence of vesicles for the solution passed through the filter. This protocol corrects for the loss of PNPB on the filter.

An independent estimate of the value of the partition coefficient was also obtained by the measurement of the solubility limit monitored as a change in the scattering in the presence of a constant amount of POPG. The amount of solute partitioned into the interface and the solubility limit in the aqueous phase were obtained from the plot of the apparent solubility limit as a function of POPG concentration (Figure 4B).

Binding of S146A tlTGL to POPG Vesicles by RET. Binding of S146A to POPG vesicles containing 2.5 mol % HDNS was determined by fluorescence energy transfer from the four tryptophan residues of the mutant to the dansyl acceptor of HDNS at the interface (*22*). Vesicles (19 μM lipid) in 1.4 mL of 10 mM Tris at pH 8.0 were titrated with

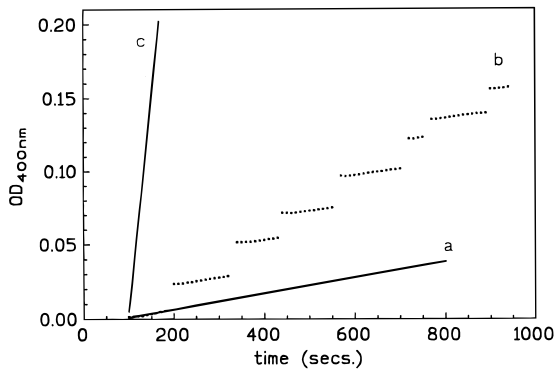

FIGURE 1: The reaction progress, monitored as the change in optical density at 400 nm, for the hydrolysis of 0.07 mM PNPB by 0.125 μg of tlTGL in 0.7 mL of 10 mM Tris at pH 8.0: (curve a) PNPB alone in unstirred solution; (curve b) as in curve a, but the cuvette was vigorously hand-shaken for 5 s at the points of discontinuity; (curve c) as in curve a, but in the presence of 0.054 mM POPG vesicles. The reaction progress seen in the presence of POPC was virtually the same as in curve a.

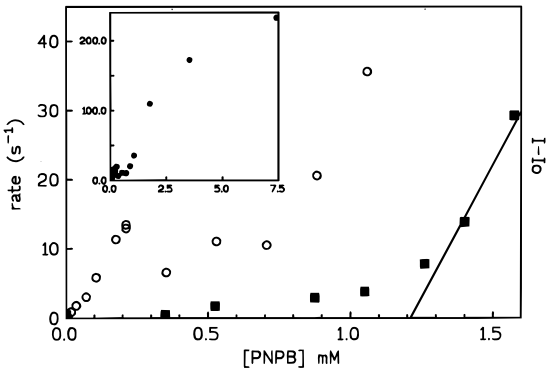

FIGURE 2: Dependence of the rate of hydrolysis on [PNPB] by tlTGL (open circles) without any additive. Closed squares show the change in the 90° scattering ($I - I_o$) with [PNPB] which corresponds to the measurement of solubility limit of about 1 mM. The plot in the inset represents the rate of hydrolysis over a wider range of [PNPB] in the reaction mixture.

the mutant in magnetically stirred solution on an SLM-Aminco AB2 spectrofluorimeter with excitation at 280 nm and emission at 495 nm with 4-nm slit widths. Data are expressed as $\delta F = (F - F_o)/F_o$, where F is the fluorescence intensity in the presence of enzyme, and F_o is the intensity in the absence of added enzyme (Figure 8).

Determination of K_d. The dissociation constant for the enzyme bound to POPG vesicles, K_d, was calculated from the hyperbolic binding isotherm obtained by monitoring the change in the fluorescence emission from the (four) tryptophan residues of S146A tlTGL at 320 nm (excitation, 280 nm) as a function of the bulk POPG concentration (Figures 9 and 10). Results are expressed as $\delta F = (F - F_o)/F_o$, where F is the fluorescence intensity in the presence of POPG, and F_o is the intensity in the absence of added lipid.

RESULTS

The Rate of Hydrolysis of PNPB Increases in the Presence of Added Anionic Vesicles. The effects of two types of interfaces on the observed rate of hydrolysis of PNPB below its solubility limit by tlTGL are shown in Figure 1. A modest rate of hydrolysis is seen in unstirred but properly mixed solution (curve a), and the rate increases dramatically in the presence of 0.05 mM POPG vesicles (curve c). A most intriguing observation is shown in curve b, where a burst of hydrolysis occurs during the vigorous shaking of the contents of the cuvette by hand. Note that the apparent rate during the mixing phase, judged from the step changes in the OD, is of the magnitude of the rate seen in the presence of POPG (curve c). Once the vigorous shaking is stopped, the rate is virtually the same as in the absence of the interface (curve a). Since the increased hydrolysis is seen only during vigorous mixing, it is attributable to the partitioning of the enzyme and substrate to the interface of the air bubbles. The possibility that the step change is due to a scattering change from the air bubbles is ruled out by the fact that the OD is stable with time after the mixing is stopped. Similar, yet more persistent, problems due to air bubbles are encountered in the pH-stat assay of the hydrolysis of tributyrin.

The rate of hydrolysis of monodisperse substrate below its solubility limit by tlTGL is sensitive to the reaction conditions. For example, mechanical stirring in the pH-stat assay creates an air−water interface of unknown area and stability, possibly in the form of bubbles and air pockets around the stirring rod and the electrode. This is probably the rationale for the use of gum arabic as an emulsifier in the pH-stat assays (*19*), i.e., to stabilize the emulsion froth of air bubbles. Therefore, even a modest observed rate of hydrolysis of monodispersed substrate (Figure 1) can only be taken as an upper limit estimate for the rate via the monodisperse ES complex (Scheme 1). In our spectroscopic assay we have minimized such complications by the use of a polished quartz cuvette and by mixing the contents by gentle 180° vertical swirls along a horizontal axis.

As summarized in Figure 2, on the basis of the results with gently mixed, unstirred solutions, we conclude that the rate of hydrolysis of PNPB below its solubility limit by tlTGL is less than 12 s^{-1}. On the other hand, as shown in the inset of Figure 2, the rate of hydrolysis exceeds 250 s^{-1} at 7.5 mM PNPB with an abrupt increase in the rate at the solubility limit. As also shown in Figure 2 (solid squares), the maximum solubility of PNPB in the aqueous buffer at pH 8.0 is 1.2 mM. The low rate below the solubility limit of PNPB shows considerable noise with a possible departure from a hyperbolic dependence on the substrate concentration. As also shown in the inset, the rate of hydrolysis of PNPB above its solubility limit increases from <12 s^{-1} to more than 250 s^{-1}, and rates depend on the method of dispersal and the solvent used for the dispersal. These results essentially confirm the observations of Martinelle et al. (*23*) on tlTGL, and they provide a lower limit estimate of the extent of rate enhancement at the interface due to intrinsic uncertainties in defining the surface area of the precipitated PNPB or in ensuring the monodisperse state of the substrate without a well-defined interface. We did not further characterize kinetics with precipitated PNPB alone.

POPG Vesicles Provide a Well-Controlled Interface for the Partitioning and Hydrolysis of PNPB or TB by tlTGL. Having demonstrated the need for an analytically useful interface for the kinetic characterization of lipolysis by tlTGL, we explored several possibilities. As shown in Figure 1, complications due to uncontrolled interfaces are virtually eliminated in the presence of POPG vesicles as the diluent surface where interfacial turnover occurs. Also, comparable or lower rates were obtained with several other anionic

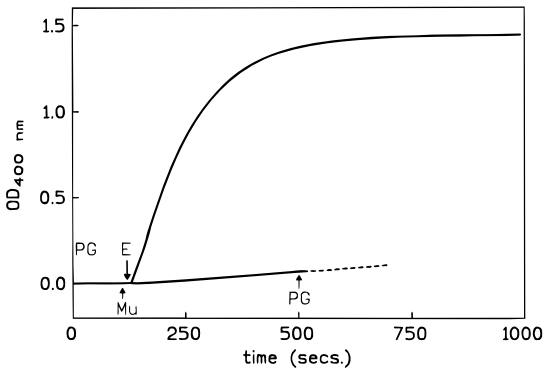

FIGURE 3: Reaction progress curves for the hydrolysis (top) of 0.07 mM PNPB in the presence of 0.054 mM POPG initiated by the addition of 0.125 μg of WT tlTGL (marked with an arrow at E) or (bottom) of 1.76 mM PNPB by 1 μg of S146A mutant tlTGL alone or after the addition of 0.054 mM POPG (dotted line after the arrow at PG).

phospholipids. These protocols showed that POPC (Figure 1) and other zwitterionic or neutral lipid dispersions do not support the hydrolysis. Although we are still investigating the structural basis for such differences, it appears that the bound enzyme may exist in the catalytically active (open) or inactive (closed) form, and the equilibrium between these two forms may be determined by the nature of the interface. However, on the basis of results described below, we believe that tlTGL on POPG vesicles is essentially completely in the active or open form to which a substrate molecule can bind. This assertion is consistent with the fact that the maximum measured rate of hydrolysis of PNPB is equal to or better than the rates seen with other assays.

As shown in Figure 3, the rate of hydrolysis of PNPB increases over 100-fold in the presence of 0.05 mM POPG vesicles, and all the available substrate is hydrolyzed at the end of the reaction progress. On the other hand, virtually no hydrolysis is seen with S146A tlTGL in the absence (0.18 s^{-1}) or presence of POPG (0.3 s^{-1}). Independent controls by the pH-stat titration method confirmed that POPG is not hydrolyzed by tlTGL. Independent pH-stat results also showed that the rate of hydrolysis of tributyrin or PNPB increases significantly in the presence of POPG. Although the maximum rates of hydrolysis of PNPB seen in both of the assays are virtually the same, the rate in the absence of POPG is noticeably higher in the pH-stat assay, presumably an artifact of vigorous mechanical stirring.

POPG provides an interface for the hydrolysis of PNPB via serine-146 at the consensus catalytic site. Kinetics of the tlTGL-catalyzed reaction on PNPB partitioned in POPG was analyzed in detail. In terms of Scheme 1, as developed in section C of Appendix, as a diluent surface POPG vesicles play two main roles: to provide the surface for the partitioning of the substrate from the aqueous phase and to provide the surface for the binding of tlTGL in the active form so that the catalytic turnover occurs at the interface. The equilibrium dissociation constant for the bound enzyme in the E* form, K_d, is defined as the diluent concentration at which half of the total enzyme is bound to the interface. Methods to measure K_d are described below.

Partitioning of PNPB in POPG vesicles is characterized by the dissociation constant K_S', defined by eq A4 in section A of Appendix; it is the diluent concentration at which half

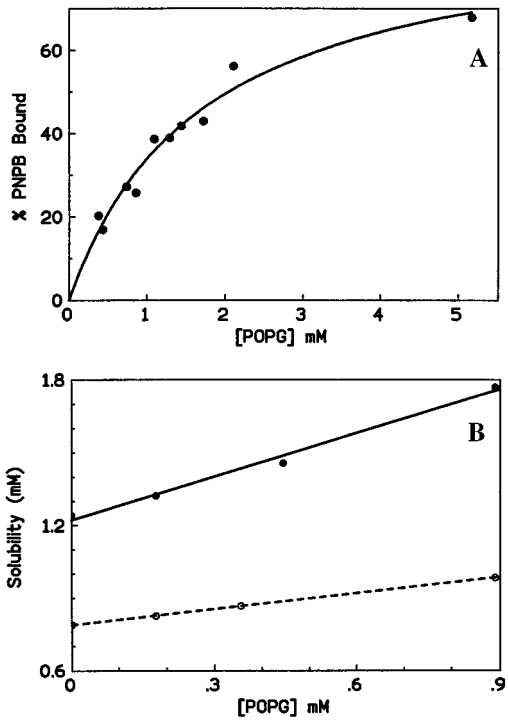

FIGURE 4: (A) Fraction (%) of 0.28 mM PNPB bound to POPG vesicles as a function of increasing concentration of POPG. (B) Change in the maximum solubility (measured as shown in Figure 2 by monitoring the abrupt change in the 90° scattering at 500 nm) of PNPB (closed circles) or tributyrin (open circles) as a function of [POPG]. The *y*-intercept gives the solubility limit for the solute in the aqueous phase, and the slope is related to φ. See text for details.

of the total substrate, except that which is precipitated, is distributed in the interface. To determine K_S', the fractional partitioning of 0.28 mM PNPB was monitored as a function of POPG concentration. An independent estimate of the aqueous solubility limit and the partitioning of the solute in POPG vesicles is provided by the results in Figure 4B. The solute in the aqueous phase, S, is in equilibrium with S*, the solute in the interface, and S_X, the aggregated or precipitated solute above its solubility limit:

Scheme 2

$$S_X \rightleftarrows S \rightleftarrows S^*$$

As in Scheme 1, S* is the solute partitioned into the POPG interface, and its concentration, X_S, is determined by K_S' (eq A4). The plot of [PNPB] versus 90° scattering in the presence of POPG shows a sharp change in the slope (not shown) comparable to that shown in Figure 2 for PNPB in the absence of POPG (squares). A straightforward interpretation of these results is possible if we assume that the break point at the start of the steep increase represents the solubility limit, where the aqueous phase and the POPG interface are saturated with the solute. Beyond this point excess solute, S_X, is precipitated to give a sharper increase in the scattering. Based on eq A11, the *y*-intercept of the plot in Figure 4B gives the solubility limits, S_{aq}^{max}, of 1.22 mM for PNPB and 0.79 mM for tributyrin. Similarly, the slope gives $X_S^{max} = 0.37$ for PNPB and 0.15 for TB. Also, eq A7 relates these two parameters to K_S'.

The solubility and partitioning parameters put a physical limit on the maximum solute mole fraction that can be

Table 1: Interfacial Kinetic Parameters for the Hydrolysis of PNPB or Tributyrin by tlTGL on a POPG Interface[a]

conditions	φ	K_S' (mM)	K_M* (mol fraction)	k^*_{cat} (s^{-1})	K_d (mM)
		PNPB			
Figure 4, panels A (eqs A9 and A11) and B (eq A7)	−1	2.0			
Figure 5 (eqs A9 and A21)	(−1)	(2.0)	0.42	2600	(0.05)
Figure 7 (eqs A9 and A21)	(−1)	(2.0)	0.38	2000	(0.05)
Figure 10					0.057
		Tributyrin			
Figure 4B	(0)	5.3			
Figure 5 analogue	(0)	(5.3)	0.047	3900	(0.05)
Figure 6	(0)	(5.3)	0.017		(0.05)

[a] Values in parentheses were used as constants for the calculations.

incorporated in the POPG bilayer, which provides significant insights into the nature of the underlying equilibria involved in the steady-state catalytic turnover. This analysis is critical for the evaluation of the mole fraction of a sparingly soluble substrate in the interface that the bound enzyme "sees". Stated simply, as related by K_S', a sparingly soluble solute partitions into the aqueous phase and the POPG interface. However, excess solute, beyond the maximum solubility in the aqueous phase and the interface, is precipitated in the S_X form.

As shown in Figure 4A, the percent PNPB bound to POPG vesicles was adequately fitted to eqs A9 and A11. Together with the results in Figure 4B, this gives $K_S' = 2.1$ mM and $\varphi = -1$. Note that the K_S' values for PNPB and TB are larger than their maximum solubility limits (Table 1). A possible basis for this is developed in section A of Appendix. The difference is attributed to the relative interfacial area contributed by the solute versus POPG. This is parametrized as φ (eq A5) to include differences in the areas of the solute and the diluent, and also as a first-order approximation for other nonidealities. In fact, a traditional method to account for such nonidealities of a solution is through the activity factor, which in this case is given by $1/(1 + \varphi X_S)$. For an ideal mixture of solute in the interface, $\varphi = 0$ and the activity factor is 1. Positive φ values, resulting from surface compensation or the solute-enhanced binding of the solute, will give activity coefficients less than 1. On the other hand, negative φ values, resulting from repulsive solute−solute interactions which decrease the partitioning of additional solute, will give activity coefficients greater than 1. From the results in Figure 4, the estimated $\varphi = -1$ for PNPB suggests repulsive interactions or a negligible surface area contribution. For the lack of conclusive results for TB, we assume that $\varphi = 0$. As shown below, these results are consistent with the kinetic results, which depend on X_S.

Effect of POPG on the Steady-State Rate of Hydrolysis of PNPB. The dependence of the observed rate on [PNPB] at 0.05 mM POPG is shown in Figure 5. As developed in section C of Appendix, under these conditions two processes are at work. Below its solubility limit, PNPB partitions only in the interface, and as related by K_S' (eq A15), X_S increases with [PNPB]; above the solubility, limit precipitated excess solute forms its own interface. Thus, X_S and the observed rate do not increase above the solubility limit. The enzyme could be distributed between POPG vesicles and the S_X interface; however, the plateau above the solubility limit in

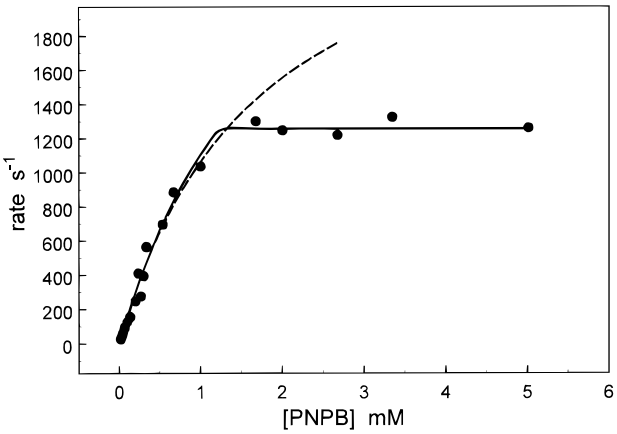

FIGURE 5: Dependence of the initial rate of hydrolysis by tlTGL on PNPB concentration in the presence of 0.05 mM POPG. The K_M^{app} and V_M^{app} parameters were obtained by curve fitting to a hyperbola (dashed line). The solid line was fit to eqs A9 and A21 with fixed $\varphi = -1$, $K_S' = 2.0$, and $K_d = 0.05$ mM to obtain $K_M^* = 0.42$ mol fraction and $k^*_{cat} = 2600$ s^{-1}.

Figure 5 is consistent with the conclusion that the enzyme remains substantially bound to POPG vesicles.

$$K_M^{app} = \frac{K_M^*\,(K_S' + [ND])}{(1 + K_M^*)}\left(1 + \frac{1}{K_{ND}^*} + \frac{K_d}{[ND]}\right) \quad (1)$$

$$v_o = k^*_{cat}\frac{X_S}{X_S + K_M^*} \quad (2)$$

$$\frac{v_1}{v_2} = 1 + \frac{\dfrac{S_2}{K_M^{\,2}}}{1 + \dfrac{S_1}{K_M^{\,1}}} \quad (3)$$

The hyperbolic fit for the points below the solubility limit is shown in Figure 5 (dashed line), which gives two apparent parameters, $K_M^{app} = 1.7$ mM and $V_M^{app} = 2900$ s^{-1}. Although the apparent parameters can be analyzed to obtain primary kinetic and equilibrium parameters (eq A23), this hyperbolic approximation is valid only at low X_S and not all the way up to the saturation level where $X_S = 0.37$. Also, only using the data points at low X_S makes it difficult to adequately resolve K_M^* and k^*_{cat}. Thus, a more rigorous analysis was carried out. According to eqs A21 and A9, the dependence of the rate on the total [S] in the reaction mixture is expressed in terms of K_d, K_S', K_M^*, k^*_{cat}, and K_{ND}^*. Since K_S' and K_d are determined independently, and since $K_{ND}^* \geq 1$ for reasons described later, the fit (smooth line) shown in Figure 5 provides values of the primary interfacial kinetic parameters $K_M^* = 0.42$ mol fraction and $k^*_{cat} = 2600$ s^{-1} for PNPB (Table 1).

As a competitive substrate, tributyrin lowers the rate of hydrolysis of PNPB. As developed in section D of Appendix and shown in Figure 6, the behavior is as expected for a competitive inhibitor. According to eq A29 recast as eq 3, the concentration of tributyrin for 50% inhibition of PNPB hydrolysis, $I_c(50) = 0.24$ mM, is related to the apparent K_M^1 for PNPB and the apparent K_M^2 for TB. The value of K_M^2 for TB calculated from the inhibition results is 0.17 mM using $K_M^1 = 0.8$ mM, compared to $K_M^2 = 0.48$ mM obtained

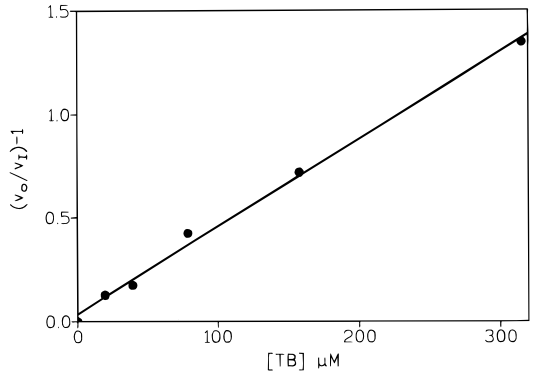

FIGURE 6: Apparent inhibition of the hydrolysis of 0.353 mM PNPB (v_o) by tlTGL in the presence of 0.053 mM POPG and increasing concentrations of tributyrin (v_I). The $I_c(50)$ obtained from this plot is related by eq 3 to $K_M^{app} = 0.17$ mM for tributyrin and $K_M^{app} = 0.8$ mM for PNPB (Figure 5). $K_M^{app} = 0.46$ mM was obtained independently by the pH-stat titration of tributyrin under the conditions of Figure 5.

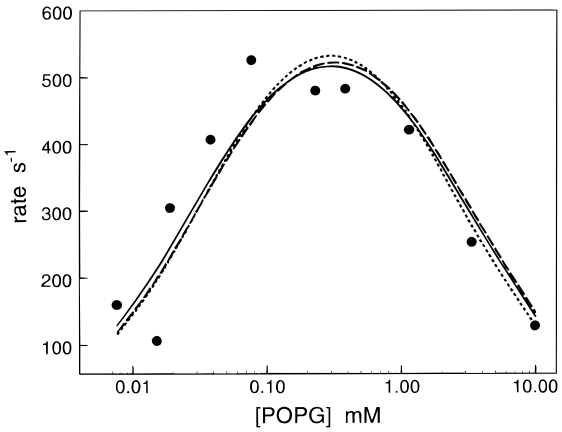

FIGURE 7: Dependence of the initial rate of hydrolysis of 0.353 mM PNPB by tlTGL on the POPG concentration. Conditions were as in Figures 1 and 3. The solid line is a best fit of the data points to eqs A9 and A21 using fixed $\varphi = -1$, $K_d = 0.05$ mM, $K_S' = 2.0$ mM, and $K_{ND}^* \gg 1$ to obtain $K_M^* = 0.4$ mol fraction and $k^*_{cat} = 2000$ s^{-1}. The dashed line is a best fit to the hyperbolic approximation, eq A23, which gives $K_M^* = 0.5$ mol fraction and $k^*_{cat} = 2900$ s^{-1}. To impress the covariance in the various parameters, the dotted line shows a best fit to eqs A9 and A21 where $K_M^* = 1$ mol fraction is also fixed to give $k^*_{cat} = 4500$ s^{-1}. The fit could not be improved by letting other parameters float. Systematic error in the low concentration range is possibly due to an additional contribution from the rate at the cuvette surface.

by the pH-stat titration. The difference between the K_M^2 values obtained by the two methods is above the expected error range. If the difference is real, such a nonideality may be expected to result if TB and PNPB each interfere with the solubility of the other; however, it is likely that the K_M^2 obtained by the pH-stat method is an artifact of the background rate due to stirring.

Dependence of the initial rate of hydrolysis of 0.35 mM PNPB as a function of [POPG] is shown in Figure 7. Under these conditions, X_S is below 0.15 through the whole concentration range and the hyperbolic relation eq A23 is expected to hold fairly well. The location of the peak in Figure 7 is determined primarily by the external parameters K_S' and K_d, eq A25, both of which provide a control on the rate. A best fit (dashed line) with eq A23 keeping $K_S' = 2.0$ mM, $K_d = 0.05$ mM, and $K_{ND}^* \gg 1$ fixed gives $K_M^* = 0.5$ mol fraction and $k^*_{cat} = 2700$ s^{-1}. Using the more general relations in eqs A21 and A9 gives a best fit (solid line) for $K_M^* = 0.4$ mol fraction and $k^*_{cat} = 2000$ s^{-1}. However, since all data in this set are at low X_S, there is a very large covariance between K_M^* and k^*_{cat} in these estimates, and one gets an almost equally good fit (dotted line) using, for example, $K_M^* = 1$ mol fraction and $k^*_{cat} = 4500$ s^{-1}. If K_d is also allowed to float, the best fit is for $K_d = 0.04$ mM, $K_M^* = 0.5$ mol fraction, and $k^*_{cat} = 2300$ s^{-1}.

The concern whether POPG is a perfect diluent can be addressed at this stage, and the resuults are consistent with $K_{ND}^* > 1$. The maximum rates measured on dispersions in gum arabic are about 2000 s^{-1} (*18*, *25*). Assuming that the mole fraction of the substrate is the maximum possible $X_S = 1$, estimated k^*_{cat} will be 3000 s^{-1} (eq 2). Of course, this is a lower limit estimate because X_S could be lower. The k^*_{cat} values on POPG (Table 1) are 50% higher than those on gum arabic, which suggests that POPG is a significantly better diluent than gum arabic for the kinetic measurements.

Results at hand also show that $K_{ND}^* \gg K_M^*$. For the fits in Figures 5 and 7 and Table 1, we have used $K^*_{ND} \gg 1$ mol fraction. According to eq 1, a lower value would not significantly change the uncertainty in the fit, except that the estimated value of K_M^* would change in the same direction. Beside the fact that the assumption of $K_{ND}^* > 1$ is consistent with the observed kinetic results, the rationale for the use of POPG as an effective diluent also comes from other observations. For example, in Figure 2 (inset) the maximum observed rate at the interface of PNPB ($X_S = 1$) is at best lower than the observed maximum rate in Figures 5 and 7, where $X_S < 0.5$ mol fraction. Also among the various phospholipid and detergent dispersions that we have tested, POPG gave the maximum rate of hydrolysis.

As described next, the direct binding studies with the catalytically inert S146A mutant give $K_d = 0.057$ mM, which is consistent with the values estimated from the kinetic studies with WT under the kinetic conditions. A correspondence between the spectroscopic and kinetic K_d values also suggests that $K_{ND}^* > 1$ mol fraction. Since the active site occupancy is a step sequential to the binding of the enzyme to the interface (Scheme 1), these results suggest either that POPG does not bind to the active site of both of the proteins or that WT and the mutant bind POPG to the active site with the same affinity. This is consistent with the assumption of $K_{ND}^* \geq 1$, and we are exploring ways to independently confirm it. As discussed later, the underlying problem is far from trivial because a diluent must bind the enzyme to the interface in an active, or open, form without occupancy of the active site. Obviously, at present it is not posisble to measure the fraction of the bound enzyme that may remain in the "closed" form under a given set of conditions.

Binding of tlTGL to POPG Vesicles. Evidence for the interaction of S146A tlTGL with POPG vesicles comes from the resonance energy transfer signal resulting from the tryptophan donors of the mutant to the dansyl-lipid acceptor at the interface. As shown in Figure 8, the RET intensity at 490 nm increases with the amount of protein added, and the intensity reaches a maximum when the surface is essentially covered with the protein. On the basis of the RET distance of about 15 Å, the 2.5-fold increase in the intensity corresponds to a donor−acceptor separation of less than 10 Å (Jain and Vaz, 1987).

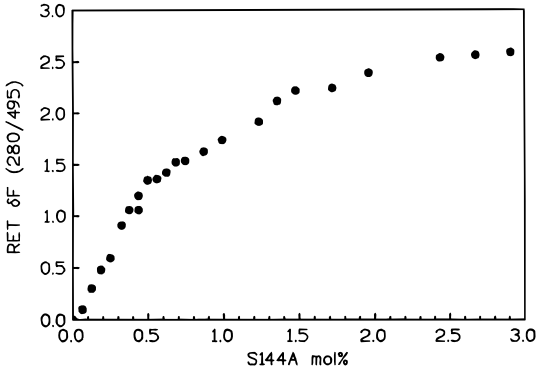

FIGURE 8: Change in the resonance energy transfer intensity at 490 nm (excitation, 280 nm) resulting from the addition of S146A mutant tlTGL to 19 μM POPG vesicles containing 2.5% HDNS (N-dansylated hexadecylphosphoethanolamine).

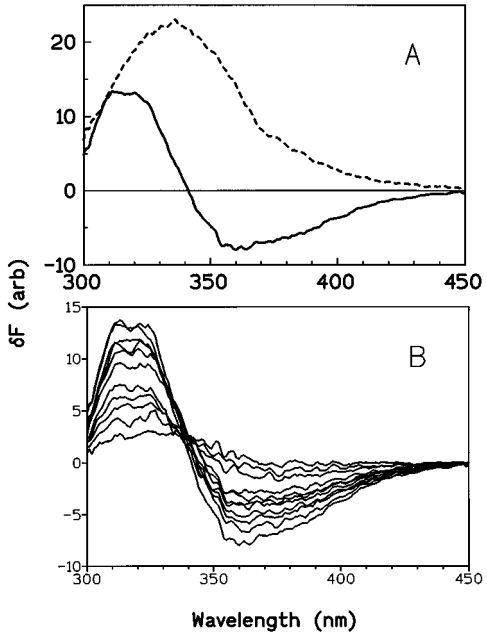

FIGURE 9: Change in the fluorescence emission spectra (excitation, 280 nm) of 50 μg (1.19 μM) of S146A mutant tlTGL in 1.4 mL of 10 mM Tris at pH 8.0. (A) Change on the addition of (solid line) 0.135 mM POPG or (dashed line) 1.5 mM POPC. (B) Change as a function of [POPG] with the maximum values plotted in Figure 10.

An independent measure of the binding of S146A to POPG vesicles was obtained by monitoring the change in the tryptophan fluorescence emission. Such changes, associated with the binding of WT and mutant, showed a remarkable variation in the spectral signatures. For example, as shown in Figure 9A, depending on the charge on the interface, the bound protein could exist in different forms on POPC and POPG. For detailed studies we chose the conditions that closely mimic the kinetic results. As shown by the difference spectra (Figure 9B) as a function of [POPG], the binding of S146A is accompanied by an increase in the emission intensity at 320 nm and a decrease at 360 nm. These spectra are noisy because a low concentration of enzyme was used, which permits measurement of K_d values in the lower range of POPG concentrations. A well-defined isobestic point suggests that the fluorescence change is due to a one step equilibrium as implied in E to E*. The change in the intensity at 320 nm shows a hyperbolic dependence on [POPG] with a maximum change in the intensity of 32%

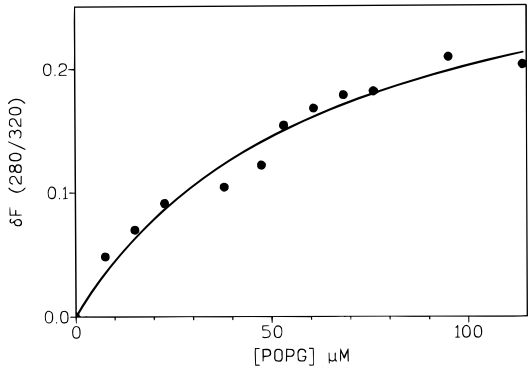

FIGURE 10: Change in the Trp fluorescence emission intensity at 320 nm (from the results in Figure 9) as a function of [POPG]. The hyperbolic fit gave $K_d = 57$ μM.

(Figure 10). As compared in Table 1, $K_d = 0.057$ mM obtained from this fit is in accord with values of K_d from the kinetic results in Figures 5 and 7. According to the argument in section B in Appendix, the hyperbolic fit assumes that the excluded surface area effect is negligible. Also note that the K_d values as defined here correspond to the total (inside + outside) number of POPG molecules, so the real K_d value is about half the number estimated.

Comparable Kinetic Behavior Is Observed with Pancreatic Lipase. Several commercially available triglyceride lipases hydrolyze PNPB in the presence of phospholipid vesicles. For example, enzymes from pig pancreas, *Candida*, and *Pseudomonas* spp. showed noticeable rate enhancement in the presence of anionic phospholipids. Analysis similar to that in Figure 7 showed that, for the pig pancreatic triglyceride lipase, the rate enhancement for the hydrolysis of PNPB is not seen in the presence of zwitterionic phospholipid. However, in the presence of anionic dimyristoylphosphatidylmethanol vesicles, for the pig lipase the observed rate increases about 50-fold, with $K_d = 30$ μM, $K_M^* = 0.4$ mol fraction, and $k^*_{cat} = 25$ s^{-1} for PNPB. Detailed studies were not carried out because the preparations (from Sigma) were quite impure and the isoenzymes were not resolved.

DISCUSSION

At a very fundamental level, Scheme 1 follows from the kinetic scheme which we developed to account for the hydrolysis of phospholipid vesicles and micelles by phospholipase A_2 (*2, 10, 11, 24*). This paradigm for the analysis of interfacial catalysis emphasizes the challenge of identification and characterization of the microscopic equilibrium and steady-state conditions that the bound enzyme sees. Now we have extended the limits of analysis to include a rapidly exchangeable substrate that partitions into the preexisting interface. Results show that the problem of understanding the control of catalysis by lipase at the interfaces can be quantitatively described by using rapidly exchanging substrates partitioned on well-defined interfaces of bilayer vesicles. Such conditions eliminate or reduce the possible number of uncontrolled variables to a point that the steady-state kinetics can be characterized in terms of primary parameters with well-established functional significance.

Interfacial Kinetics with Exchangeable Substrate. In this study we exploited the broad substrate specificity of tlTGL to quantitatively characterize its interfacial catalytic behavior in terms of the primary rate and equilibrium constants of

well-defined functional significance. The assay is well suited for the study of the catalytic mechanism and activation of interfacial enzymes on well-defined interfaces. Of course, the working range for X_S is limited by K_M*, K_S', and the solubility limit.

Partitioning of a solute in the interface is related to K_S,′ and thus K_S' determines the mole fraction of the substrate that the bound enzyme sees during the steady state. As indicated earlier (Scheme 2) and in section A of the Appendix, the solubility limit for a sparingly soluble solute in the aqueous phase establishes the maximum mole fraction of the substrate in the interface, X_S^{max}. If the interface does not undergo a phase change, excess solute beyond this limit would form its own phase and thus be excluded from the aqueous phase as well as the diluent interface.

Several sources of nonideality in the interfacial solution behavior of a solute partitioned in the interface are expected. Often dilute solutions are ideal, and the activity factor controls the problems arising from the compensating or repulsive solute−solute and solute−solvent interactions. As a first approximation, the area factor φ is useful to account for the possible reasons that make K_S' different from the solubility limit in water. In addition, $\varphi = -1$ for PNPB suggests that its partitioning decreases with increasing X_S. Although it does not appear to be the case here, it is conceivable that the partitioning of certain solutes could induce a major organizational change in the bilayer, and thus discontinuities would be seen in the substrate concentration dependence.

Diluent for Lipase. It is clear that the use of a diluent is absolutely critical for a quantitative analysis of interfacial catalysis and activation in terms of the primary rate and equilibrium processes intrinsic in Scheme 1. Recall that, according to our original conceptualization (*25*), a diluent must provide an interface for the partitioning of the substrate and the enzyme and that the molecules of the diluent must not bind to the active site. Yet another consideration emerges in applying this concept to lipase. As discussed later, unlike secreted phospholipase A_2, lipases have a structural feature that may act as a lid to cover the active site. Thus in the conceptualization of a diluent for lipase, one strives for a diluent on which the bound lipase is present with an open lid, or an active conformation that accepts the substrate according to the $E^* + S \rightleftarrows E^*S$ equilibrium for the formation of the Michaelis complex. We are not absolutely sure if we have achieved a 100% open form of the E* state for tlTGL on POPG, but we do believe that at least a large proportion of the bound enzyme is present in the active form or it is readily converted to the active form in the presence of the substrate. Obviously, this is not the case for the enzyme bound to POPC vesicles, where no significant rate of hydrolysis is seen.

Scheme 1 as a General Kinetic Paradigm for Lipase. Lipolytic enzymes constitute a large group of industrially and biologically important ester hydrolases (*16, 26*−*30*). The natural substrates of lipase have poor solubility in water, and thus lipolytic activity of tlTGL makes it an effective additive in laundry detergent (*18*). The family of lipolytic enzymes includes enzymes with a broad range of specificities for the substrate as well as the interfaces. For example, secreted phospholipase A_2 is exceedingly specific for the *sn*-2-acyl ester bond of phospholipid (*1*). On the other hand, *Aeromonas* lipase shows esterolytic activity toward glyceride and phospholipid, as well as the acyl transferase activity (*29, 31, 32*).

Our kinetic analysis should be helpful in resolving some of the outstanding problems of lipase kinetics. Despite early breakthroughs (*26, 33, 34*), kinetic studies with triglyceride lipase have suffered from a wide range of problems. These originate mostly from the inability to present the enzyme with a suitable interface in which the distribution of the substrate and enzyme can be quantitatively ascertained during the assay. Equally perplexing and acute has been the problem of presenting an interfacial enzyme with a soluble monodisperse substrate, because amphiphilic solutes partition on the walls of reaction vessel, as well as at the air−water interface of air bubbles. Such variables have not been adequately controlled before (*35*). Also, the use of a monolayer of glyceride at the air−water interface (*19, 30*) or as mixed micelles (*36*) has not yielded interpretable interfacial kinetic parameters. This is not surprising. Using the experience with phospholipase A_2 as a guide (*2, 12, 36*), backed with good theoretical reasons (*10, 11*), it is quite likely that on many of these interfaces the rate-limiting step is shifted from the interfacial catalytic turnover to some other step such as substrate replenishment or the removal of the product from the microenvironment of the bound enzyme. In short, interfacial kinetics cannot be meaningfully interpreted to establish primary rate and equilibrium constants unless it can be assured that the microscopic steady state in the microenvironment of the bound enzyme is satisfied (*10, 11*). Under the fast exchange conditions established in the assay used for the present study, the bulk concentrations with the reaction progress faithfully represent the local concentration seen by the enzyme at the interface.

Cationic Residues in the Hinge Control the Interfacial Activation. Protocols developed in this study are helpful in quantitatively assigning functional roles for specific structural features of tlTGL. A lack of activity with the S146A mutant confirms a consensus role for the serine in the chemical step. Since the catalytic turnover by tlTGL is seen only in the presence of POPG, and not POPC, vesicles, we suggest that the lid covering the active site, seen in the X-ray structure of tlTGL (*14, 15, 37, 38*), moves to the open position due to interactions of cationic residues in the hinge region of the lipase with the anionic headgroups of POPG vesicles.

tlTGL belongs to a subfamily of lipases isolated from a wide range of microorganisms (*14, 16*). These lipases contain 250−320 residues. In tlTGL the catalytic triad consists of Asp-201, His-258, and Ser-146 in the sequence GHSLG. tlTGL shows 32% sequence identity and virtually identical three-dimensional structure with the *Rhizomucor miehei* lipase (rmTGL). The crystal structure of tlTGL at 3.25-Å resolution shows considerable similarity to rmTGL in the catalytic site region (*21*). In both cases the catalytic site lined with hydrophobic residues is buried under a lid of a two-turn (residues 86−93) amphiphilic α-helix containing Trp-89 on the hydrophobic face, and Ser-83 and Asp-96 are believed to serve as pivots:

$$F_{80}\mathbf{R}GS\mathbf{R}S\underline{IENWI}_{90}\underline{GNL}NFDL\mathbf{K}EI_{100}$$

Since tlTGL is not active at zwitterionic interfaces, a possible contribution of the lower dielectric constant (*39*) is not

sufficient for lid opening, although it may stabilize the open form. In fact, such effects associated with interactions along the lid-containing hydrophobic face may trap the enzyme in the closed form at the interface.

We propose that the lid helix swings open on the binding of the enzyme to the anionic interface; that is, certain cationic residues must control the lipid opening. Note that several residues on both sides of the lid are in the exposed loop that connects β-turns 3 and 4. A modest change in the Trp-emission spectrum on the binding of S146A tlTGL to POPG vesicles (Figures 9 and 10) suggests that the change associated with the binding is due to a change in the environment of Trp-89 on the lid. Useful information about the hinge region can be deduced from the available results. Note that the enhanced hydrolysis of PNPB by tlTGL is not seen in the presence of zwitterionic POPC vesicles (Figure 2). Although tlTGL binds to POPC vesicles, the spectral changes are qualitatively different from those seen with POPG (Figures 9A). This fact alone suggests that electrostatic interactions are a critical part of the lid opening at the interface. Cationic residues in the hinge region on both sides of the lid that could play such a role include residues K73, R80, R83, and K97. In E form these residues could act as electrostatic "locks" on the hinge.

The idea of a hinge controlled by an electrostatic lock provides a conceptual basis for the enhanced hydrolysis seen with pancreatic triglyceride lipase, which shows enhanced hydrolysis of tributyrin and PNPB at anionic but not zwitterionic interfaces. On the basis of the consensus 237−261 lid domain, it appears that K232, K249, and R265 could act as the cationic lock (*14*, *40*). Since there is very little direct functional evidence for these assertions, we believe that the kinetic methods developed here in conjunction with site-directed mutagenesis are suited to provide conclusive evidence for the electrostatically controlled lid for the activation of lipase at the interface.

APPENDIX

Interfacial Hydrolysis of Substrate That Does Not Form Its Own Interface

(A) Equilibrium Interfacial Binding of Substrate. The interface is built up from molecules of neutral diluent, ND, and substrate, S. For simplicity, it is assumed that ND molecules are not water soluble and that all are in the interface. The concentration of substrate molecules that partition into the interface is assumed to be proportional to the area, A^*, of the interface and determined by an interfacial dissociation constant K_S'' from

$$K_S'' = \frac{[A^*][S_{aq}]}{[S^*]} \tag{A1}$$

Square brackets denote concentration per unit volume of the aqueous phase; $[S_{aq}]$ and $[S^*]$ are the concentrations of substrate in the aqueous phase and interface, respectively, and $[A^*]$ is the surface area of interface per unit aqueous phase volume. If a_N and a_S denote the surface area that each ND and S molecule, respectively, contributes to the interface area, we can write

$$[A^*] = a_N[ND^*] + a_S[S^*] = [ND^*]a_N\left\{1 + \frac{X_S}{1 - X_S}\frac{a_S}{a_N}\right\} \tag{A2}$$

where the mole fraction of substrate in the interface is defined as

$$X_S = \frac{[S^*]}{[ND^*] + [S^*]} \tag{A3}$$

This gives

$$\frac{X_S}{[S_{aq}]} = \frac{a_N}{K_S''}\left\{1 + X_S\left(\frac{a_S}{a_N} - 1\right)\right\} = \frac{1}{K_S'}(1 + \varphi X_S) \tag{A4}$$

where the area correction factor is

$$\varphi = \frac{a_S}{a_N} - 1 \tag{A5}$$

$K_S' = K_S''/a_N$ is the dissociation constant per mole of interface molecules for the substrate from an interface with $X_S = 0$, or with $a_S = a_N$ as we have defined it before (*11*, *12*). At equilibrium the mole fraction of substrate in the interface is

$$X_S = \frac{[S_{aq}]}{K_S' - \varphi[S_{aq}]} \tag{A6}$$

If S has a limited solubility corresponding to $[S_{aq}^{max}]$, then from eq A6 the maximum mol fraction of S in the interface is given by

$$X_S^{max} = \frac{[S_{aq}^{max}]}{K_S' - \varphi[S_{aq}^{max}]} \tag{A7}$$

or $X_S^{max} = 1$, whichever is smaller.

The area correction factor, φ, introduced above accounts for a possible influence from unequal surface areas of the interface molecules. When $\varphi \approx 0$, the equilibrium relation (A6) simplifies to that used previously (*11*, *12*). It is quite possible, however, that other nonideal effects also contribute to interface binding. For example, substrate could bind more or less easily to the interface depending on the amount of substrate already present. If such effects are present, binding would be dependent on X_S, and φ should be considered as a first-order correction for such contributions as well. In fact, $1/(1 + \varphi X_S)$ is the activity factor for substrate in the interface.

Since X_S is not a primary variable, it is more convenient to transform to the total concentration of substrate added to the system, [S]:

$$[S] = [S^*] + [S_{aq}] = [S^*] + K'_S X_S/(1 + \varphi X_S) \tag{A8}$$

From eqs A3 and A8 we can eliminate $[S^*]$ and solve for X_S:

$$X_S = {}^1/_2\left(\frac{K_S' + [S] + [ND^*] - \varphi[S]}{K_S' - \varphi([S] + [ND^*])}\right) \pm {}^1/_2\left[\left(\frac{K_S' + [S] + [ND^*] - \varphi[S]}{K_S' - \varphi([S] + [ND^*])}\right)^2 - \frac{4[S]}{K_S' - \varphi([S] + [ND^*])}\right]^{1/2} \quad (A9)$$

which simplifies to

$$X_S = {}^1/_2\left(\frac{K_S' + [S] + [ND^*]}{K_S'}\right) - {}^1/_2\left[\left(\frac{K_S' + [S] + [ND^*]}{K_S'}\right)^2 - \frac{4[S]}{K_S'}\right]^{1/2} \quad (A10)$$

when $\varphi = 0$.

The fraction of substrate bound to the interface can be calculated as

$$\frac{[S^*]}{[S]} = 1 - \frac{[S_{aq}]}{[S]} = 1 - \frac{X_S K_S'}{[S](1 + \varphi X_S)} \quad (A11)$$

Inserting eq A9 for X_S, this has been plotted in Figure 4A as a function of [ND*]. A best fit with the experimental data for PNPB in POPG suggests that φ is between -2 and 5 and the corresponding K_S' values are between 1.8 and 3.1 mM. The solubility as a function of added ND in Figure 4B has a slope which is $[S^*]/[ND^*] = X_S^{max}/(1 - X_S^{max})$. For PNPB, this gives $X_S^{max} = 0.37$. Inserting this value and the solubility $[S_{aq}^{max}] = 1.2$ mM in eq A7, one finds that $K_S' = 3.2 + 1.2\varphi$. However, to satisfy all the data of Figure 4, we must choose $K_S' = 2.0$ and $\varphi = -1$. As an area correction factor, $\varphi = -1$ implies that the addition of S to the interface does not change its total surface area, eq A5. As a general nonideality factor, a negative value of φ suggests that the interactions for S in the interface make it increasingly difficult to add more S at large X_S. The shape of the curve in Figure 4A suggests that the first-order activity factor is sufficient for X_S up to ca. 0.15. The interpretation above requires that it is valid also up to the maximum $X_S^{max} = 0.37$.

Similarly, for tributyrin the results of Figure 4B, give a solubility of 0.79 mM and $X_S^{max} = 0.15$; thus from eq A7 the relationship $K_S' = 5.3 + 0.8\varphi$ should hold. For this substrate there is no result corresponding to Figure 4A, and the parameters cannot be determined independently. However, since X_S is always small, the nonideal correction does not matter so much in this case and the choice $\varphi = 0$, $K_S' = 5.3$ is the simplest. Other choices for φ between -1 and 1 have little effect on the interpretation of the kinetic results.

(B) Equilibrium Interfacial Binding of Enzyme. Similarly, it can be assumed that enzyme binds to the interface in proportion to the surface area of the interface, corresponding to a dissociation constant

$$K_d'' = \frac{[A^*][E_{aq}]}{[E^*]} \quad (A12)$$

Together with eq A2, this gives the equilibrium relation

$$\frac{[E^*]}{[E_{aq}]} = \frac{a_N}{K_d''}[ND^*]\left\{1 + \frac{X_S}{1 - X_S}\frac{a_S}{a_N}\right\} = \frac{[ND^*](1 + \varphi_d X_S)}{K_d(1 - X_S)} \quad (A13)$$

where $[E_{aq}]$ and $[E^*]$ denote the concentrations of enzyme in solution and in the interface, respectively. $K_d = K_d''/a_N$ is the dissociation constant per mole of molecules in the interface when all molecules contribute equally (*11*, *12*). φ_d is the area correction factor defined as in eq A4. However, to the extent that this factor includes other nonideal effects, it may well be different for the surface binding of S and of E.

These relations are valid when the ratio of bound enzyme to lipid is very small, as is the case in the kinetic studies reported above. When enzyme coverage of the interface becomes large, excluded surface and packing effects will also contribute to the binding isotherm. Figure 10 shows the binding curve as a function of increasing interface [ND*] when no substrate is present. Surprisingly, the shape of this experimental curve is hyperbolic even at low [ND*] when enzyme coverage is expected to be significant. This suggests that excluded surface effects are compensated possibly by favorable enzyme−enzyme interactions in the interface.

(C) Steady-State Rate of Interfacial Hydrolysis. From Scheme 1 we pick out the following main reactions:

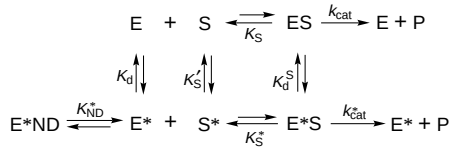

(A14)

It is assumed that the neutral diluent (ND) may have some affinity for the active site and therefore could work as an inhibitor, with dissociation constant K^*_{ND} in the interface. It is further assumed that ND is all in the interface. If substrate and produce exchange between neutral diluent particles and solution is much faster than catalytic turnover, all steps prior to E*S formation can be considered equilibrated:

$$[S_{aq}] = \frac{K_S' X_S}{1 + \varphi X_S} \quad (A15)$$

$$[E^*] = \frac{[E_{aq}][ND^*](1 + \varphi_d X_S)}{K_d(1 - X_S)} \quad (A16)$$

$$[E^*ND] = \frac{[E^*]X_{ND}}{K^*_{ND}} = \frac{[E^*](1 - X_S)}{K^*_{ND}} \quad (A17)$$

Equations A15 and A16 are from eqs A6 and A13. Since we have introduced an activity factor, $1/(1 + \varphi X_S)$, for the interface concentration X_S, this must also influence the equilibrium of S* to E*S so that the detailed balance condition for the equilibrium binding in Scheme 1 remains satisfied. It appears likely that the activity factor will influence the S* to E*S binding also under catalytic conditions so that the amount of E*S complex is determined by the Michaelis constant, K_M^*, as

$$[E^*S] = \frac{[E^*]X_S}{K^*_M(1 + \varphi X_S)} \quad (A18)$$

Similarly, the amount of ES complex in solution is determined by the corresponding Michaelis constant, K_M, as

$$[ES] = \frac{[E_{aq}][S_{aq}]}{K_M} = \frac{[E^*]K_d(1 - X_S)K_S'X_S}{K_M[ND^*](1 + \varphi X_S)(1 + \varphi_d X_S)} \quad (A19)$$

In the second equality, $[S_{aq}]$ and $[E_{aq}]$ from eqs A15 and A16 have been replaced. At equilibrium (i.e., when $k^*_{cat} = k_{cat} = 0$), the Michaelis constants should be replaced by the equilibrium constants, K_S^* and K_S of Scheme 1. Equations A18 and A19 require for their validity that ES ↔ E*S exchange is slow (11).

The steady-state rate of hydrolysis per enzyme can be calculated as

$$v = \frac{k^*_{cat}[E^*S] + k_{cat}[ES]}{[E^*S] + [E^*] + [E^*ND] + [E_{aq}] + [ES]} \quad (A20)$$

Through eqs A16−A19, the concentrations of all enzyme species are related to [E*], and they an be replaced in eq A25 (below) to give the steady-state rate as a function of X_S and [ND*]. (Apart from the area correction φ, this is equivalent to the result given in eq A5 of ref *11* if I is replaced by ND and no EI species in solution is considered. While it is possible to use eq A5 of ref *11* to write the equation for the rate of hydrolysis also in the case where ND can bind E in solution, the result is considerably more complicated and is not needed for this study.)

Equations A16−A20 together with A9 completely define the rate as a function of the total [ND*] and [S]. When catalysis in solution contibutes significantly, the turnover will go through a maximum at low [S] and then decrease at higher substrate concentrations. In the limit when ES complexes in solution do not contribute significantly (i.e., when K_M is very large), the result can be further simplified to

$$v = \frac{k^*_{cat}X_S}{X_S + K_M^*(1 + \varphi X_S)\left\{1 + \frac{1 - X_S}{K_{ND}^*} + \frac{K_d(1 - X_S)}{(1 + \varphi_d X_S)[ND^*]}\right\}} \quad (A21)$$

As long as the mole fraction, X_S, of substrate in the interface is much smaller than 1, eq A9 can be approximated as

$$X_S \approx \frac{[S]}{K_S' + [ND^*] + [S](1 - \varphi)} \quad (A22)$$

Including only first-order contributions from X_S in eq A21 and replacing X_S by eq A22 gives the rate expressed in terms of the total concentrations of S and ND:

$$v = \frac{k^*_{cat}[S]}{[S](1 + K_M^*) + K_M^*(K_S' + [ND^*])\left(1 + \frac{1}{K_{ND}^*} + \frac{K_d}{[ND^*]}\right)} \quad (A23)$$

For simplicity, $\varphi_d = 0$ has been assumed as well. This is a hyperbolic relation for v vs [S] that can be written in a standard Michaelis−Menten form as

$$v = \frac{V_M^{app}[S]}{[S] + K_M^{app}} \quad (A24)$$

V_M^{app} and K_M^{app} can be identified in terms of the primary constants as given by eqs 1 and 2 in the main text. Equations A23 and A24 can be applied only for small $X_S < X_S^{max}$. Significant departures from the Michaelis−Menten relation can be expected when the mole fraction of substrate in the interface is not much smaller than 1 or when $X_S = X_S^{max}$ (see Figure 5); in this case, the full eq A21 should be used together with eq A9.

If v is studied vs [ND*] at constant [S], eq A23 will go through a maximum at

$$[ND^*]_{max} = \sqrt{\frac{K_S'K_d}{1 + 1/K_{ND}^*}} \quad (A25)$$

When [ND*] is small, not enough protein is bound; when [ND*] is large, the substrate in the interface becomes too dilute and the rate goes down in both limits (cf. Figure 7).

(D) Competititve Substrates. Consider the case where two different substrates, S1 and S2, can partition into an interface of ND. The euilibrium distribution of substrates will be given by

$$[S1_{aq}] = \frac{K_{S1}'X_{S1}}{1 + \varphi_1 X_{S1} + \varphi_2 X_{S2}} \quad (A26a)$$

$$[S2_{aq}] = \frac{K_{S2}'X_{S2}}{1 + \varphi_1 X_{S1} + \varphi_2 X_{S2}} \quad (A26b)$$

in obvious notations and in analogy with eq A4. Combining these equations with the mass balance relations,

$$[S1] = [S1^*] + [S1_{aq}] = \frac{X_{S1}[ND^*]}{1 - X_{S1} - X_{S2}} + \frac{K_{S1}'X_{S1}}{1 + \varphi_1 X_{S1} + \varphi_2 X_{S2}} \quad (A27a)$$

$$[S2] = [S2^*] + [S2_{aq}] = \frac{X_{S2}[ND^*]}{1 - X_{S1} - X_{S2}} + \frac{K_{S2}'X_{S2}}{1 + \varphi_1 X_{s1} + \varphi_2 X_{S2}} \quad (A27b)$$

gives approximately (to first order in X_{S1} and X_{S2})

$$X_{S1} \approx \frac{[S1]/([ND^*] + K_{S1}')}{1 + \frac{(1 - \varphi_1)[S1]}{[ND^*] + K_{S1}'} + \frac{(1 - \varphi_2)[S2]}{[ND^*] + K_{S2}'}} \quad (A28a)$$

$$X_{S2} \approx \frac{[S2]/([ND^*] + K_{S2}')}{1 + \frac{(1 - \varphi_1)[S1]}{[ND^*] + K_{S1}'} + \frac{(1 - \varphi_2)[S2]}{[ND^*] + K_{S2}'}} \quad (A28b)$$

These approximations are valid only when the mole fractions

in the interface of both substrates are much smaller than 1 and smaller than X_S^{max}.

For simplicity, assume that ES1 and ES2 complexes in solution can be neglected; then the steady-state rate of hydrolysis of S1 per enzyme in the presence of the competing substrate S2 can be written from eq A21 as

$$v_1^{(2)} = (k^*_{cat} X_{S1}/K_{M1}^*) \Bigg/ \left\{ \frac{X_{S1}}{K_{M1}^*} + (1 + \varphi_1 X_{S1} + \varphi_2 X_{S2}) \times \left\{ 1 + (1 - X_{S1} - X_{S2}) \left(\frac{1}{K_{ND}^*} + \frac{K_d}{[ND^*]} \right) \right\} + \frac{X_{S2}}{K_{M2}^*} \right\} \quad \text{(A29)}$$

The extra term in the denominator accounts for the amount of enzyme present as E*S2 complex. Taking only first order contributions from X_{S1} and X_{S2}, and introducing the approximate relations from eqs A28a,b, the rate in eq A29 can be more compactly expressed as

$$v_1^{(2)} = \frac{V_{M1}^{app}[S1]}{K_{M1}^{app} + [S1] + [S2]K_{M1}^{app}/K_{M2}^{app}} \quad \text{(A30)}$$

where V_{M1}^{app} and K_{M1}^{app} are the apparent Michelis−Menten parameters (eqs 1 and 2 in the main text) for S1 in the absence of S2, and K_{M2}^{app} is for S2 in the absence of S1. Thus, in this limit, the competing substrates behave exactly as expected in the usual solution kinetics. Deviations from this standard result may occur when substrates in the interface are not at low mole fractions, or when contributions from ES1 or ES2 complexes in solution also are significant.

REFERENCES

1. Verheij, H. M., Slotboom, A. J., and de Haas, G. H. (1981) *Rev. Physiol. Biochem. Pharmacol. 91*, 91−203.
2. Jain, M. K., Gelb, M. H., Rogers, J., and Berg, O. G. (1995). *Methods Enzymol. 249*, 567−614.
3. Gelb, M. H., Jain, M. K., Hanel, A. M., and Berg, O. G. (1995) *Annu. Rev. Biochem. 64*, 653−688.
4. Thunnissen, M. M. G. M., Ab, E., Kalk, K. H., Drenth, J., Dijkstra, B. W., Kuipers, O. P., Dijkman, R., de Haas, G. H., and Verheij, H. M. (1990) *Nature 347*, 689−691.
5. Scott, D., White, S. P., Otwinowski, Z., Yuan, W., Gelb, M. H., and Sigler, P. B. (1990) *Science 250*, 1541−1546.
6. Scott, D., and Sigler, P. (1994). *Adv. Protein Chem. 45*, 53−88.
7. Dupureur, C. J., Yu, B. Z., Jain, M. K., Noel, J. P., Deng, T., Li, Y., Byeyon, I. L., and Tsai, M. D. (1992) *Biochemistry 31*, 6402−6413.
8. Dupureur, C. J., Yu, B. Z., Mamone, J. A., Jain, M. K., and Tsai, M. D. (1992) *Biochemistry 31*, 10576−10583.
9. Sekar, K., Yu, B. Z., Rogers, J., Lutton, J., Liu, X., Chen, X., Tsai, M. D., Jain, M. K., and Sundaralingam, M. (1997) *Biochemistry 36*, 3104−3114.
10. Berg, O. G., Yu, B.-Z., Rogers, J., and Jain, M. K. (1991) *Biochemistry 30*, 7283−7297.
11. Berg, O. G., Rogers, J., Yu, B.-Z., Yao, J., Romsted, L. S., and Jain, M. K. (1997) *Biochemistry 36*, 14512−14530.
12. Jain, M. K., Yu, B. Z., and Berg, O. G. (1993) *Biochemistry 32*, 11319−11329.
13. Yu, B. Z., Ghomashchi, F., Cajal, Y., Annand, R. R., Berg, O. G., Gelb, M. H., and Jain, M. K. (1997) *Biochemistry 36*, 3870−3881.
14. Derewenda, Z. S. (1994). *Adv. Protein Chem. 45*, 1−52.
15. Derewenda, U., Swenson, L., Green, R., Wei, Y., Dodson, G. G., Yamaguhci, S., Haas, M. J., and Derewenda, Z. S. (1994) *Nature Struct. Biol. 1*, 36−39.
16. Woolley, P., and Petersen, S. B., Eds. (1994) *Lipases−Their Structure, Biochemistry and Application*, p 363, Cambridge University Press, Cambridge.
17. Thirstrup, K., Verger, R., and Carriere (1994) *Biochemistry 33*, 2748−2756.
18. Svendsen, A., Clausen, I. G., Patkar, S. A., Borch, K., and Thellersen, M. (1997) *Methods Enzymol. 284*, 317−340.
19. Gargouri, Y., Bensalah, A., Douchet, I., and Verger, R. (1995) *Biochim. Biophys. Acta 1257*, 23−229.
20. Verger, R. (1997). *Trends Biotechnol. 15* (January), 32−38.
21. Lawson, D. M., Brzozowski, A. M., Dodson, D. D., Hubbard, R. E., Huge-Jensen, B., Boel, E., and Derewenda, Z. S. (1994) In *Lipase*, pp 77−94, Cambridge University Press, Cambridge.
22. Jain, M. K., and Vaz, W. L. C. (1987) *Biochim. Biophys. Acta 906*, 1−8.
23. Martinelle, M., Holmquist, M., and Hult, K. (1995) *Biochim. Biophys. Acta 1258*, 272−276.
24. Jain, M. K., Rogers, J., Jahagirdar, D. V., Marecek, J. F., and Ramirez, F. (1986) *Biochim. Biophys. Acta 860*, 435−447.
25. Jain, M. K., Ranadive, G. N., Rogers, J., Yu, B. Z., and Berg, O. G. (1991) *Biochemistry 30*, 7306−7317.
26. Borgstrom, B., and Brockman, H. L. (1984) *Lipase*, p 527, Elsevier, Amsterdam.
27. Waite, M. (1987) *Phospholipase*, Plenum Press, New York.
28. Mackness, M. I., and Clerc, M., Eds. (1994) *Esterases, Lipase, and Phospholipase: from Structure to Clinical Significance*, p 279, Plenum Press, New York.
29. Hilton, S., and Buckley, J. T. (1991) *Biochemistry 30*, 6070−6074.
30. Deveer, A. M. Th. J., Dijkman, R., Leuveling-Tjeenk, M., Van der Berg, L., Ransac, S., Batenberg, M., Egmond, M., Verheij, H., and DeHaas, G. H. (1991) *Biochemistry 30*, 10034−10042.
31. Upton, C., and Buckley, J. T. (1995) *Trends Biochem. Sci. 20*, 178−179.
32. Jain, M. K., Krause, C. D., Buckley, J. T., Bayburt, T., and Gelb, M. G. (1994) *Biochemistry 33*, 5011−5020.
33. Sarda, L., and Desnuelle, P. (1958) *Biochim. Biophys. Acta 30*, 513−521.
34. Desnuelle, P., Sarda, L., and Ailhard, G. (1960) *Biochim. Biophys. Acta 37*, 570−571.
35. Ferrato, F., Carriere, F., Sarda, L., and Verger, R. (1997) *Methods Enzymol. 286*, 327−347.
36. Sugihara, A., Gargouri, Y., Pieroni, G., Riviere, C., Sarda, L., and Verger, R. (1986) *Biochemistry 25*, 3430−3434.
37. Derewenda, U., Brzozowski, A. M., Lawson, D. M., and Derewenda, Z. S. (1992) *Biochemistry 31*, 1532−1541.
38. Cygler, M., and Schrag, J. D. (1997) *Methods Enzymol. 284*, 3−27.
39. Norin, M., Olsen, O., Svendsen, A., Edholm, O., and Hult, K. (1993) *Protein Eng. 6*, 855−860.
40. van Tilbeurgh, H., Egloff, M. P., Martinez, C., Rugani, N., Verger, R., and Cambillau, C. (1993) *Nature 362*, 814−820.

BI972998P